Draft version June 1, 2009
Preprint typeset using LaTeX style emulateapj v. 11/12/01

A CHANDRA VIEW OF NGC 3621: A BULGELESS GALAXY HOSTING AN AGN IN ITS EARLY PHASE?

Mario Gliozzi
George Mason University, 4400 University Drive, Fairfax, VA 22030

Shobita Satyapal
George Mason University, 4400 University Drive, Fairfax, VA 22030

Michael Eracleous[1]
Department of Astronomy & Astrophysics and Center for Gravitational Wave Physics, The Pennsylvania State University, 525 Davey Lab, University Park, PA 16802

Lev Titarchuk
NASA Goddard Space Flight Center, Code 662, Greenbelt, MD 20771
George Mason University, 4400 University Drive, Fairfax, VA 22030

Chi C. Cheung
Astrophysics Science Division, NASA Goddard Space Flight Center, Greenbelt, MD 20771
Draft version June 1, 2009

ABSTRACT

We report the detection of a weak X-ray point source coincident with the nucleus of the bulgeless disk galaxy NGC 3621, recently discovered by *Spitzer* to display high ionization mid-infrared lines typically associated with AGN. These *Chandra* observations provide confirmation for the presence of an AGN in this galaxy, adding to the growing evidence that black holes do form and grow in isolated bulgeless disk galaxies. Although the low signal-to-noise ratio of the X-ray spectrum prevents us from carrying out a detailed spectral analysis of the nuclear source, the X-ray results, combined with the IR and optical spectroscopic results, suggests that NGC 3621 harbors a heavily absorbed AGN, with a supermassive black hole (SMBH) of relatively small mass accreting at a high rate. *Chandra* also reveals the presence of two bright sources straddling the nucleus located almost symmetrically at $20''$ from the center. Both sources have 0.5–8 keV spectra that are well-fitted by an absorbed power-law model. Assuming they are at the distance of NGC 3621, these two sources have luminosities of the order of 10^{39} erg s^{-1}, which make them ultra-luminous X-ray sources (ULXs) and suggest that they are black hole systems. Estimates of the black hole mass based on the X-ray spectral analysis and scaling laws of black hole systems suggest that the 2 bright sources might be intermediate mass black holes with $M_{\rm BH}$ of the order of a few thousand solar masses. However, higher quality X-ray data combined with multi-wavelength observations are necessary to confirm these conclusions.

Subject headings: Galaxies: active – Galaxies: nuclei – X-rays: galaxies

1. INTRODUCTION

The well-known correlation between the black hole mass, $M_{\rm BH}$, and the host galaxy stellar velocity dispersion $\sigma_\star$ (Gebhardt et al. 2000; Ferrarese & Merritt 2000) implies that black hole growth and the build-up process of galaxy bulges are closely related. The fact that the vast majority of AGNs reside in galaxies with prominent bulges (e.g. Heckman 1980; Ho, Filippenko, & Sargent 1997; henceforth H97) suggests that bulges play a critical role in the formation and growth of nuclear black holes. However, exceptions do exist, the most notable example being NGC 4395, a nearby Sd galaxy that lacks a bulge and shows optical and X-ray properties typical of a Seyfert 1 galaxy (e.g., Filippenko & Ho 2003; Moran et al. 2005) with an inferred black hole mass of 3.6×10^5 M$_\odot$ (Peterson et al. 2005), much less massive than black holes found in galaxies with massive bulges. Until recently, this galaxy was an anomaly in that it was the only essentially bulgeless disk galaxy to harbor a nuclear black hole. It furthermore contains a nuclear star cluster (Filippenko & Ho 2003), providing a unique opportunity to study the connection between nuclear star clusters and black holes. More recently, Greene & Ho (2004; 2007) searched the Sloan Digital Sky Survey for galaxies with similar intermediate mass black holes and found more examples of broad-line AGNs, many of which reside in disk-dominated galaxies that lack a classical bulge. Other more nearby examples of AGNs or AGN candidates in late-type galaxies have been found based on infrared, optical, and X-ray studies (Satyapal et al. 2008; Shields et al. 2008; Ghosh et al. 2008; Barth et al. 2008; Thornton et al. 2008; Dewangan et al. 2008; Desroches & Ho 2009). Although these studies demonstrate that AGNs reside in late-type disk galaxies, NGC 4395 remains exceptional since it is both near enough for detailed study and is a truly bulgeless disk galaxy

The investigation of AGNs in bulgeless galaxies is important for the following reasons. First, it can shed light on the connection between black holes and galaxy formation and evolution, by addressing the following outstanding questions: How does the black hole mass and accretion

[1] Center for Gravitational Wave Physics, The Pennsylvania State University, University Park, PA 16802

rate relate to the properties of the parent galaxy in the case of bulgeless galaxies? Second, since bulgeless galaxies are thought to be in an early phase of their evolution, they allow us to probe the mechanisms for growth of supermassive black holes which are still poorly known. Constraints on the low-mass end of the black hole mass function provide the best discriminant among models that predict the evolution of black holes from extremely high redshifts to the present time (e.g., Volonteri, Lodato, & Natarajan 2008). But before we can carry out any of the above tests, we have to locate the black holes themselves.

The search for weak nuclear activity associated with black holes in extremely-late type normal galaxies is observationally challenging because these galaxies are typically dusty and have significant star formation rates. Therefore, such a search is best carried out in energy bands that do not suffer from heavy dust or gas extinction and in which contaminating emission from star-forming regions is relatively weak. Thus, the mid-IR and hard X-ray bands are well suited for this purpose and, in fact, studies in these two bands complement each other well.

Observations of the mid-IR fine structure lines provide us with one of the few definitive tools for discovering buried AGNs in dusty galaxies. AGNs show prominent high excitation fine structure lines whereas starburst and normal galaxies are characterized by lower excitation spectra characteristic of H II regions ionized by young stars (e.g. Genzel et al. 1998; Sturm et al. 2002; Satyapal et al. 2004). One of the key prominent lines is the [Ne V] 14μm line, which cannot be produced in H II regions surrounding young stars, the dominant energy source in starburst galaxies, since even hot massive stars emit very few photons with energy sufficient for the production of this ion. The power of these diagnostics in finding buried AGNs has been convincingly demonstrated by the discovery of a population of AGNs in galaxies that display optically "normal" nuclear spectra (e.g., Satyapal et al. 2004).

Once the presence of an AGN is ensured via IR spectroscopy, X-ray observations represent the most effective means to investigate the AGN properties, since: 1) The X-rays are produced and reprocessed in the inner, hottest nuclear regions of the source. 2) The penetrating power of (hard) X-rays allows them to carry information from the central engine without being substantially affected by absorption, and to probe the presence of the putative torus (provided that $N_{\rm H} < 10^{24}$ cm^{-2}). 3) Compared to optical and UV radiation, X-rays are far less affected by host galaxy contamination.

Using high resolution IRS observations from the *Spitzer* archive, Satyapal et al. (2007, 2008) started to investigate the IR spectral properties of late-type (Sc or later) galaxies. Remarkably, of the 33 late-type galaxies with no definitive signatures of AGNs in the optical, 8 display [Ne V] emission. This result suggests that AGNs might be common not only in early-type galaxies but also in late-type ones, extending the ubiquity of the AGN phenomenon in the local Universe. In their sample of galaxies showing robust evidence for a [Ne V] line, NGC 3621 ($z = 0.0024$) is unique in that, like NGC 4395, it does not show evidence of any bulge component, it contains a nuclear star cluster (Barth et al. 2009) and is the closest one, with a distance of 6.6 Mpc bulgeless galaxies based on Cepheid measurements (Freedman et al. 2001). Very recently, Barth et al. (2009), using high quality optical spectra through a small aperture, detected a Seyfert 2 emission-line spectrum, supporting the hypothesis that NGC 3621 harbors an accreting supermassive black hole. Additionally, the measurement of the stellar velocity dispersion provided an upper limit for the black hole mass of 3×10^6 M$_\odot$. X-ray observations can strengthen the case for presence of an accreting black hole in this galaxy and allow us to determine some of the basic properties of the system, such as the ionizing luminosity and the accretion rate, given an estimate of the black hole mass.

Here, we report the first X-ray study of NGC 3621 based on a 25 ks *Chandra* observation. The primary goal of this project is to verify whether this galaxy harbors an accreting supermassive black hole. As explained below, our *Chandra* observation reveals the presence of 2 additional bright X-ray sources located $\sim$20$''$ from the center. Therefore, a secondary goal of this work is to investigate the nature of these 2 enigmatic X-ray sources.

The outline of the paper is as follows. In § 2 we describe the observations and data reduction. The X-ray results are reported in § 3. In § 4 we discuss our findings, and in § 5 we summarize the main results and draw our conclusions.

2. OBSERVATIONS AND DATA REDUCTION

NGC 3621 was observed with *Chandra* ACIS-S on March 6, 2008. The *Chandra* data, provided by the *Chandra* X-Ray Center, were processed using `CALDB` v. 3.4.2 following standard criteria. Only events with grades 0, 2–4, and 6 and in the energy range 0.5–8 keV were retained. We also checked that no flaring background events occurred during the observations. The extraction of images, light curves, and spectra, as well as the construction of response matrices, was carried out following standard procedures. Background spectra and light curves were extracted from source-free regions on the same chip of the source. The counts were extracted from circular regions with radius of 3$''$.

The spectral analysis was performed using the `XSPEC v.12.3.0` software package (Arnaud 1996; Dorman & Arnaud 2001). For the brightest source, the spectra were re-binned in order to contain at least 15 counts per channel, which is appropriate for the use of the χ^2 statistic. For the second off-nuclear source, given the low number of counts, we used the Cash statistic (Cash 1979) to fit the un-binned spectra over an energy range of 0.5–8 keV (in the observer's reference frame), where the calibration is best known (Marshall et al. 2005) and the background negligible. The errors on spectral parameters are at 90% confidence level for one interesting parameter ($\Delta\chi^2,\ \Delta C = 2.71$).

3. RESULTS

Chandra, with its sub-arcsecond spatial resolution, is the best X-ray satellite to investigate the spatial distribution of the X-ray emission. This is crucial for AGN studies and specifically for detection of weak AGNs, since these are typically associated with compact un-resolved regions as opposed to starburst activity, which instead is characterized by extended emission (e.g., Dudik et al. 2005; González-Martín et al. 2006; Flohic et al. 2006).

Figure 1 shows the *Chandra* contours overlaid with the *Spitzer* IRAC 3.6μm image of the NGC 3621 galaxy from the SINGS survey (Kennicutt et al. 2003). The nuclear X-ray source shows a clear correspondence with the IR peak. Figure 2 shows the *Chandra* ACIS-S image of NGC 3621 overlaid with 1.4 GHz contours obtained from a VLA[2] snapshot observation at 20″ resolution (160 s, archival program AC345). The nuclear X-ray source (hereafter source A, marked by a black box) is located at the center of the image.

Interestingly, two bright off-nuclear X-ray sources are detected at ∼20″ from the center. While no clear IR association is evident for the 2 X-ray off-nuclear sources, the brighter X-ray source B may have a radio counterpart in the VLA map with a peak of 5.2 mJy/beam that is ∼4″ offset (to the north of) the X-ray source. At D=6.6 Mpc, the corresponding 1.4 GHz radio luminosity is 3×10^{26} erg s^{-1} Hz^{-1} for an assumed point source. At the position of the X-ray nucleus and source C, the radio map is dominated by diffuse emission from the galaxy and the formal 1σ upper limits are 3.9 mJy/beam and 4.9 mJy/beam (the radio surface brightnesses at the X-ray position), corresponding to point source limits of $\lesssim (2-3) \times 10^{26}$ erg s^{-1} Hz^{-1}. A higher resolution VLA 8.5 GHz snapshot (107 s, archival program AR555) did not reveal any significant emission at these locations with point source limits of 0.5 mJy (5σ) at 0.53″ × 0.22″ resolution. The vastly differing resolutions of the two radio maps preclude any practical constraints on the radio source spectra.

At first glance the symmetric placement of the two off-nuclear sources relative to respect to the center of the galaxy, and their apparent association with radio emission, suggests that they may be related to the central source. They resemble hot-spots produced by the interaction of bipolar outflows with the interstellar medium. However, the results of our analysis of their time-averaged X-ray spectra (see below) seem to rule out this scenario.

3.1. *Source A: The Central Source*

The X-ray central region is located at RA=11$^{\rm h}$18$^{\rm m}$16.51$^{\rm s}$, DEC=-32° 48′ 50.4″ (the coordinates here and in the rest of the paper refer to the J2000 epoch, and have been determined using the `celldetect` task in CIAO). Note that the *Chandra* position of the central source is fully consistent with the NGC 3621 coordinates from the *2MASS* catalog, RA=11$^{\rm h}$18$^{\rm m}$16.50$^{\rm s}$, DEC=-32° 48′ 50.6″ (Skrutskie et al. 2006).

Using the `CIAO` tool `dmextract`, we extracted the X-ray counts from a central circular region of radius of 1.5″ (black thick circle in Figure 3) and from 8 background regions surrounding it, as shown in Figure 3. After background subtraction, we detect 21 ± 6 X-ray counts from the source, which is significant at the 3.7 σ level. The uncertainty was calculated using the approach of Gehrels (1986), which is appropriate for a small number of counts.

Unfortunately, with such few counts, it is impossible to spectrally characterize source A; neither direct spectral fitting nor hardness ratio calculations yield useful information. Examining the morphology in several, narrow energy bands only reveals that most of the counts (∼70%) are in the energy range 0.8–1.8 keV, which coincides with the peak of the *Chandra* ACIS effective area curve. Therefore, we resort to deriving some estimates of the absorbed flux and corresponding intrinsic luminosity using the simulation tool `PIMMS`.

Assuming a power-law model with photon index Γ ranging from 1.7 to 2.0 (which is typical for AGNs) and a Galactic column density of $N_{\rm H} = 5.74 \times 10^{20}$cm^{-2}, we obtain an absorbed flux of $F_{0.5-8\,{\rm keV}} \sim 6.5 \times 10^{-15}$ erg cm^{-2} s^{-1} ($F_{2-10\,{\rm keV}} \sim 4 \times 10^{-15}$ erg cm^{-2} s^{-1}). The Seyfert 2 spectroscopic classification and the relatively large bolometric luminosity, inferred by both IR and optical studies (Satyapal et al. 2007; Barth et al. 2009), suggest the presence additional absorption, local to NGC 3621. In order to infer plausible values for the intrinsic luminosity, we assumed some additional intrinsic absorption with column densities ranging from 5×10^{21} to 5×10^{23} cm^{-2}. The lower value of $N_{\rm H}$ is consistent with the one derived from spectral fitting of the 2 off-nuclear sources (see below), whereas the upper value is a typical value found in non Compton-thick Seyfert 2 galaxies (see, e.g., Figure 3 of Bassani et al. 1999). The resulting values of the estimated luminosities, which mostly depend on the choice of intrinsic $N_{\rm H}$ (variations of Γ cause luminosity differences of the order of a few percent only) are $L_{0.5-8\,{\rm keV}} \sim 7 \times 10^{37}$ erg s^{-1} ($L_{2-10\,{\rm keV}} \sim 5 \times 10^{37}$ erg s^{-1}) and $L_{0.5-8\,{\rm keV}} \sim 3 \times 10^{39}$ erg s^{-1} ($L_{2-10\,{\rm keV}} \sim 2 \times 10^{39}$ erg s^{-1}), for the moderate and heavy absorption scenarios, respectively.

In summary, the *Chandra* observations reveal the presence of a weak point-like X-ray source at the center of NGC 3621, which confirms the presence of an AGN. However, the paucity of counts hampers the study of the nature of this source and more specifically whether this system is heavily absorbed or not.

3.2. *Source B: the Brightest Off-Nuclear Source*

Source B is fairly X-ray bright (more than 2000 counts were collected during the 20.6 ks net exposure) located at RA=11$^{\rm h}$18$^{\rm m}$15.16$^{\rm s}$, DEC=-32° 48′ 40.6″. Since Source B is much brighter than the other sources in the *Chandra* field of view, one may have the impression that its emission is spatially extended. However, a comparison of the brightness radial profile with the ACIS point spread function reveals that X-ray spatial distribution is fully consistent with that of a point-like source.

Figure 4 shows the Hubble Space Telescope (*HST*) ACS WFC images centered around the position of Source B. The position of the off-nuclear X-ray source was observed at the edge of the field of *HST* images obtained in the F435W, F555W (not shown), and F814W filters (each with 3x360s exposures; program 9492) on 2003 February 16. Aligning the X-ray and optical nucleus in the *Chandra* and *HST* images, we find a faint optical source 0.33" from the center of the X-ray position of source B, although only the eastern ∼1/2 of the X-ray error circle was covered in the WFC images. Ulitizing r=0.2" circles, we measured count rates for the optical source including four surrounding source-free regions for background estimation. The optical source is a 4.5σ detection in the F435W image, a

[2] The National Radio Astronomy Observatory is operated by Associated Universities, Inc. under a cooperative agreement with the National Science Foundation.

lower significance detection (2.8σ) in the F555W image, and is undetected in the F814W image, where 1 σ errors were determined by calculating the standard deviation of the background count rates. Count rates were converted to flux density utilizing the PHOTFLAM and PHOTPLAM keywords in the FITS header and the aperture corrections tabulated in Sirianni et al. (2005), and are reported in Table 1.

The relatively high X-ray count rate of Source B allows us to investigate not only the X-ray spectral properties via direct fitting of the spectrum but also the temporal properties. We have extracted the light curve in the 0.5–8 keV energy range, from a circular region with a radius of $3''$ centered on source B. This light curve is shown in Figure 5. Although there appear to be some low-amplitude fluctuations toward the end of the observation, according to a χ^2 test the light curve is consistent with the hypothesis that the source flux is constant during the *Chandra* pointing (χ^2/dof=24.20/22, P_{χ^2}= 0.34).

The X-ray spectrum of source B, obtained from the same extraction region as the light curve, is poorly fitted by a simple power law with Galactic absorption (χ^2/dof=154.12/112), showing a deficit at low energies indicative of additional absorption. Indeed, by leaving the column density of the absorber free to vary, a much better fit is obtained (χ^2/dof=50.47/111) with the following parameters: $N_{\rm H} = (3.4 \pm 0.6) \times 10^{21}$ cm^{-2} and $\Gamma = 2.7 \pm 0.3$. The spectrum of source B, with the best fit overlaid, and the data-to-model ratio are shown in Figure 6. The corresponding absorbed flux is $F_{0.5-8\,{\rm keV}} = 7 \times 10^{-13}$ erg cm^{-2} s^{-1} and the intrinsic luminosity, assuming that source B is located at the same distance as NGC 3621, $L_{0.5-8\,{\rm keV}} = 7 \times 10^{39}$ erg s^{-1} ($L_{2-10\,{\rm keV}} = 2 \times 10^{39}$ erg s^{-1}). We have also tried to add a thermal component (described by the XSPEC model `apec`). Although the overall fit remains acceptable (χ^2/dof=48.97/108), the spectral parameters of the thermal component (kT and abundances) remain largely unconstrained.

The large luminosity, well in excess to the Eddington limit for a neutron star, suggests that source B can be a black hole system. As a consequence, the X-ray emission is likely to be produced by the Comptonization of seed photons emitted by the underlying accretion disk. It is therefore instructive (and indeed a necessary step to constrain $M_{\rm BH}$ in this system with the method described in §4.2) to fit the *Chandra* spectrum of source B with the physically motivated `BMC` model instead of a phenomenological power law (see Titarchuk et al. 1997 for further details).

The Bulk Motion Comptonization model (BMC) is a generic Comptonization model able to describe equally well bulk motion and thermal Comptonization, although it was historically developed to describe the Comptonization of thermal seed photons by a relativistic converging flow (Titarchuk et al. 1997). The BMC model is characterized by 4 free parameters: the temperature of the thermal seed photons kT, the energy spectral index α, a parameter $\log(A)$ related to the Comptonization fraction f by the relation $f = A/(1 + A)$ (where f is the ratio of Compton scattered photons over the seed photons), and the normalization $N_{\rm BMC}$. In simple words, the BMC model convolves the thermal seed photons and a *generic* Comptonization Green's function producing a power law. As a consequence, this model adequately fits X-ray spectra of accreting black holes, which at the zeroth order are always characterized by a hard power law, which is widely believed to be produced by the Comptonization of a seed thermal component. In addition to being a comprehensive Comptonization model, the BMC model presents 2 important advantages with respect to the power law model (PL): 1) Unlike the PL, which is a phenomenological model, the BMC parameters are computed in a self-consistent way; 2) Unlike the PL, the power law produced by BMC does not extend to arbitrarily low energies and thus does not affect the normalization of the thermal component nor the amount of local absorption, which is often present around accreting objects.

The resulting best fit (χ^2/dof=49.90/110), which is statistically indistinguishable from the PL fit, yields the following parameters: $N_{\rm H} = (3.1 \pm 0.1) \times 10^{21}$ cm^{-2}, $kT = 0.1 \pm 0.1$ keV (the temperature of the seed photons), $\alpha = 1.6 \pm 0.3$ (the spectral index, which is related to the photon index by $\Gamma = \alpha + 1$), $\log A = 2$ (fixed at the best fit value), and $N_{\rm BMC} = 1.2^{+6.8}_{-0.4} \times 10^{-5}$, which is in units of $(L/10^{39}$ erg s$^{-1})(10$ kpc$/d)^2$ with L and d being the luminosity and distance of the object, respectively.

3.3. *Source C: the second off-nuclear source*

The measured X-ray position of Source C is RA=$11^{\rm h}18^{\rm m}18.23^{\rm s}$, DEC=-32° 48′ 53.0″. Figure 7 shows the *HST* ACS WFC images (described in the previous subsection) centered around the position of Source C. A faint optical source is detected 0.37" away from the *Chandra* position in all 3 filters. An additional redder source is visible 0.5" away but detected only in the F814W filter image. Additional ACS images from the HST same program obtained on Feb 3 confirm the two optical sources. The photometric results from this latter dataset are within the 1σ errors with the exception of the F435W measurement of C1 where we measure a flux that is 2σ lower than that reported in Table 1.

The moderately low X-ray count rate (∼200 counts collected during the net 20.6 ks exposure) allows a direct fitting of the un-binned spectrum using the $C-$statistics, which can be used to estimate parameters values and confidence regions but does not provide a goodness-of-fit. To this aim, on can use the `XSPEC` command `goodness` that performs Monte Carlo simulations of spectra based on the chosen model. This procedure yields the percentage of simulations with the fit statistic lower than that for the original data. If the best-fitting model is a good representation of the data the percentage should be around 50%; values $\ll$50% indicate that the data are over-parameterized, whereas values close to 100% indicate that the fit is poor.

Source C appears to be reasonably well fitted with a simple power-law model with absorption in excess to the Galactic $N_{\rm H}$ (see Figure 8), although the `goodness` command yields 74% indicating that this model is only marginally acceptable. The best fit parameters are: $N_{\rm H} = (5.1^{+2.5}_{-1.9}) \times 10^{21}$ cm^{-2} and $\Gamma = 1.6 \pm 0.4$. The corresponding absorbed flux is $F_{0.5-8\,{\rm keV}} = 1.1 \times 10^{-13}$ erg cm^{-2} s^{-1} and the intrinsic luminosity, assuming that source C is located at the same distance as NGC 3621, $L_{0.5-8\,{\rm keV}} = 7 \times 10^{38}$

erg s^{-1} ($L_{2-10\,\mathrm{keV}} = 6 \times 10^{38}$ erg s^{-1}).

Also in this case we have tried the Comptonization `BMC` model instead of a phenomenological power law. The resulting best fit parameters are: $N_{\mathrm{H}} = (5.0 \pm 2.2) \times 10^{21}$ cm^{-2}, $kT = 0.06^{+0.08}_{-0.05}$ keV, $\alpha = 0.5 \pm 0.2$, $\log A = -1.15$, $N_{\mathrm{BMC}} = (6.3 \pm 5.0) \times 10^{-6}$. The `goodness` command (98%) indicates that this model is statistically worse than the power law. However, as explained above, the results from the fitting of the `BMC` model represent the first necessary step to attempt an estimate of M_{BH} in this putative black hole system.

4. DISCUSSION

4.1. *The central source*

The primary goal of our X-ray investigation is to verify whether NGC 3621 hosts a buried AGN, as suggested by recent IR and optical spectroscopic studies. The presence of a weak X-ray source coinciding with the center of the galaxy seems to be consistent with this scenario. Unfortunately, however, the very low count rate severely hampers our investigation, preventing any X-ray spectral characterization of this source. Nevertheless, combining the *Chandra* results with findings from recent IR and optical spectroscopic studies, we may address several important questions.

Before proceeding further, it is worth summarizing the main results from longer wavelength studies that will be used in our discussion. From the IR study, we will use the bolometric luminosity, $L_{\mathrm{bol}} = 5 \times 10^{41}$ erg s^{-1}, which was derived from the $L_{[\mathrm{Ne\,V}]} - L_{\mathrm{bol}}$ correlation (Satyapal et al. 2007). From the optical investigation of Barth et al. (2009) we will make use of the following information: 1) NGC 3621 is spectrally classified as a Seyfert 2; 2) The measured [O III] λ5007 flux is $F_{[\mathrm{O\,III}]} = (22.4 \pm 0.4) \times 10^{-16}$ erg cm^{-2} s^{-1}, which, based on inspection of the two-dimensional optical line ratios, probably encompasses only 10% of the narrow line region (NRL). Note that if the last hypothesis is correct, the bolometric luminosity derived by $L_{[\mathrm{O\,III}]} - L_{\mathrm{bol}}$ correlation is fully consistent with the value inferred from $L_{[\mathrm{Ne\,V}]}$; if not, L_{bol} derived from $L_{[\mathrm{O\,III}]}$ is lower by a factor of $\sim$10.

The first outstanding question is whether the central source is heavily absorbed or intrinsically weak. Based on the *Chandra* count rate, the 2–10 keV luminosity we have inferred has a range of over 2 orders of magnitude (from a few $\times 10^{37}$ to a few $\times 10^{39}$ erg s^{-1}), depending on the adopted intrinsic N_{H} (5×10^{21} and 5×10^{23}cm^{-2}, respectively).

We can estimate the $L_{2-10\ \mathrm{keV}}$ luminosity using the $L_{[Ne\,V]}$ luminosity assuming the $L_{[Ne\,V]}/L_{2-10\ \mathrm{keV}}$ ratio in standard AGN. Using the limited number of standard AGN with both [NeV] and 2-10 keV observations (based on recent Spitzer observations of AGN from Dudik et al. 2007 and Gorjian et al. 2008), we find an average ratio of $L_{[Ne\,V]}/L_{2-10\ \mathrm{keV}} \simeq 10^{-3}$. This result, combined with the estimated value of $L_{[Ne\,V]}$ for NGC 3621, $\sim 5 \times 10^{37}$ erg s^{-1}, predicts a 2–10 keV luminosity of the order of 10^{40} erg s^{-1}, which is more than two orders magnitude greater than the observed luminosity in the weakly absorbed scenario. Therefore, this result strongly suggests that NGC 3621 is heavily absorbed.

A second indirect way to test the value of L_{X} employs the correlation between $L_{\mathrm{X}} - L_{[\mathrm{O\,III}]}$. Using the results from Mulchaey et al. (1994) for a sample of Seyfert galaxies, and, more specifically, utilizing the best-fit linear correlation derived by their Figure 3c, we obtain a luminosity of $L_{\mathrm{X}} = 9.8 \times 10^{39}$ erg s^{-1}, which is in broad agreement with the heavily absorbed scenario.

A third alternative way to constrain N_{H} (and hence L_{X}) is based on the $F_{\mathrm{X}}/F_{[\mathrm{O\,III}]} - N_{\mathrm{H}}$ diagram proposed by Guainazzi et al. (2005) and derived from the work of Bassani et al. (1999) on Seyfert 2 galaxies. In this diagram, which shows a clear anti-correlation between $F_{\mathrm{X}}/F_{[\mathrm{O\,III}]}$ and N_{H}, F_{X} is the *absorbed* 2–10 keV flux whereas $F_{[\mathrm{O\,III}]}$ is *corrected* for absorption based on the $H\alpha/H\beta$ ratio (see the appendix of Bassani et al. 1999 for details). Depending on whether $F_{[\mathrm{O\,III}]}$ encompasses 10% or the entire [O III] luminosity of the NLR, the $F_{\mathrm{X}}/F_{[\mathrm{O\,III}]}$ ratio lies between 0.1 and 1, which in turn translates into N_{H} ranging between $\sim 10^{23}$ and $\sim 10^{24}$ cm^{-2}. This result again lends support to the heavily absorbed scenario. Finally, this scenario is supported by the direct comparison between L_{X} and L_{bol}. Indeed, if we use the value obtained with moderate absorption, 5×10^{37}erg s^{-1}, we derive a bolometric correction factor of $\kappa_{2-10\,\mathrm{keV}} \equiv L_{\mathrm{bol}}/L_{2-10\,\mathrm{keV}} > 1000$, which is unreasonably high and inconsistent with any reasonable spectral energy distribution (SED) for AGNs.

Adopting the heavily obscured scenario, we can now try to constrain the most important parameters for a black hole system, namely the accretion rate, $\dot{m}$, and the black hole mass, M_{BH}. Assuming that NGC 3621 has an X-ray luminosity of few $\times 10^{39}$ erg s^{-1}, the bolometric correction factor becomes $\kappa_{2-10\,\mathrm{keV}} \gtrsim 100$. This result directly translates into an estimate the Eddington ratio value (and hence on $\dot{m}$) by virtue of the existing positive correlation between the bolometric correction factor $\kappa_{2-10\,\mathrm{keV}}$ and $L_{\mathrm{bol}}/L_{\mathrm{Edd}}$ (Vasudevan and Fabian 2009). According to Vasudevan and Fabian (2009), this bolometric correction is characteristic of systems accreting at higher rate: $L_{\mathrm{bol}}/L_{\mathrm{Edd}} \gtrsim 0.2$. This finding in turn can be used to constrain the black hole mass: Assuming that $L_{\mathrm{bol}} = 5 \times 10^{41}$ erg s^{-1}and $L_{\mathrm{bol}}/L_{\mathrm{Edd}} \simeq 0.2$, we obtain $M_{\mathrm{BH}} \simeq 2 \times 10^4$ M$_{\odot}$, which is a fairly low value and apparently below the extrapolation of the $M_{\mathrm{BH}} - \sigma$ correlation (see, e.g., Fig. 10 of Barth et al. 2009). The small M_{BH} coupled with the high $\dot{m}$ appears to be in line with the scenario where bulgeless galaxies host small supermassive black holes in their early stage that undergo a phase of very vigorous accretion, and is consistent with recent findings from Greene & Ho (2007) and Barth et al. (2008) on Seyfert 1 and Seyfert 2 galaxies, respectively.

We should point out that the scenario of a heavily absorbed AGN in NGC 3621 is not without caveats. The correlation between the [NeV] luminosity and the bolometric luminosity in standard AGN shows a scatter 0.44 dex, which corresponds to a factor of $\sim$3 uncertainty in L_{bol} derived by $L_{[\mathrm{NeV}]}$ (Satyapal et al. 2007). Furthermore, its applicability at this luminosity range is uncertain. In addition the fraction of the [OIII] luminosity encompassed by the optical spectrum obtained by Barth et al. (2009) and attributable to the AGN is also uncertain. However, taken collectively, there is strong support for the hypothesis that NGC 3621 harbors a buried AGN with luminosity

of the order of a few times 10^{41} erg s^{-1}.

4.2. *The off-nuclear sources*

The secondary goal of this work is to investigate the nature of the 2 bright off-nuclear sources detected by *Chandra*. Based on the X-ray luminosity values derived from the spectral analysis ($L_{2-10\,\mathrm{keV}} = 2 \times 10^{39}$ and 6×10^{38} erg s^{-1} for sources B and C, respectively), with the assumption that these sources are located within NGC 3621 (i.e., at a distance of 6.6 Mpc), we can already derive the first important conclusion: these are ultraluminous X-ray sources and their compact objects are likely black holes, since their X-ray luminosity exceeds the Eddington limit for neutron stars.

The lack of strong optical/UV counterparts (see Table 1), the fact that they have similar intrinsic absorption that is well in excess with respect to the Galactic value, and the apparent association with the NGC 3621 radio emission suggest that these sources are not located at significantly smaller distances than NGC 3621.

However, a priori, we cannot rule out that they are background AGN that appear to be located close to the center of NGC 3621 just by chance. To test this hypothesis, we have performed the following test. Utilizing the results of the *Chandra* spectral analysis we have derived the monochromatic X-ray luminosity $l_{2\ \mathrm{keV}}$ for different values of redshift ranging between $z = 0.05 - 1$. From the well-known tight correlation $l_{2\ \mathrm{keV}} - l_{2500\mathrm{\AA}}$ for standard AGN (we used equation 1c from Steffen et al. 2006) we have determined the corresponding values of $l_{2500\mathrm{\AA}}$ and the relative fluxes. Finally, the expected values for the flux at the wavelengths probed by the *HST* observations have been obtained by converting the 2500Å fluxes assuming a typical slope of 0.7 ($f_\nu \propto \nu^{-0.7}$).

For Source B the predicted optical flux ranges between 230–370 μJy (depending on the optical band) at $z = 0.05$ and 6-9 mJy at $z = 1$. For the weaker X-ray Source C, we obtain optical fluxes of the order 14-21 μJy at $z = 0.05$ and 345–535 μJy at $z = 1$. Since these expected values for standard AGN are at least 2 orders of magnitude larger than the measured optical fluxes reported in Table 1, we can rule out the hypothesis of background AGN. We also applied extinction corrections by assuming the absorption column density derived from the X-ray spectral fits, N_{H}, and converting it into optical extinction with the relation $A(V)/N_{\mathrm{H}} = 5.3 \times 10^{-22}$ (Cox & Allen 2000). This corresponds to $A(V)$ =1.8 and 2.7, which in turn translates into flux correction factors of ∼5 and ∼10 for source B and C, respectively. Nevertheless, the measured optical fluxes are still inconsistent with the predicted values for standard AGN.

We can therefore reasonably assume that both off-nuclear sources reside in NGC 3621. At a distance of 6.6 Mpc, the measured fluxes of their putative optical counterparts correspond to optical luminosities of the order of $\sim 10^{36} - 10^{37}$ erg s^{-1}, which, combined with the estimated X-ray luminosities, appear to be in line with typical values of $L_{\mathrm{X}}/L_{\mathrm{opt}}$ measured in X-ray binaries (e.g., Ritter & Kolb 2003). In the hypothesis that these sources are indeed hosted by NGC 3621, it is important to determine whether they are analogs of Galactic microquasars like GRS 1915+105, or intermediate black holes (IMBHs) close to the center of the galaxy.

In order to shed light on the nature of these sources, and specifically derive useful constraints on their M_{BH} and distance, we will make use of two different methods, that are based on the X-ray spectral fitting results with the `BMC` model. Both methods rely on the generally accepted assumption that the X-ray spectrum is produced by Comptonization of a thermal component associated with an accretion disk. The first method assumes a specific model for the accretion disk based on the seminal work from Shakura & Sunyaev (1973) and interpret kT as the color temperature of the accretion disk (which is related to the effective disk temperature by a "hardening factor" T_h). On the other hand, the second method only assumes that the underlying physics in black hole systems is the same irrespective of the scale. Therefore, with the second method M_{BH} can be directly derived by scaling self-similar relationships between spectral (and temporal) parameters. For further details, see Shaposhnikov & Titarchuk (2009).

The first method has been introduced by Shrader & Titarchuk (1999) and successfully applied to derive M_{BH} in several Galactic black holes (GBHs), in intermediate BHs, and also in a sample of Narrow Line Seyfert 1 galaxies (see Shrader & Titarchuk 2003 for details). The second method, on the other hand, is based on the extension of the scaling technique presented by Titarchuk & Fiorito (2004) and Shaposhnikov & Titarchuk (2007). Specifically, it is based on the universal scalable relationship between the photon index and the normalization of the `BMC` model, which appears to be characteristic of all GBHs during their spectral transitions (Shaposhnikov & Titarchuk 2009).

In simple terms, the second method can be summarized by the following steps. 1) Construct a $\Gamma - N_{\mathrm{BMC}}$ plot for a GBH of known mass and distance, which will be used as reference (hereafter denoted by the subscript r). 2) Compute the normalization ratio between the target of interest (hereafter denoted by the subscript t) and the reference object $N_{\mathrm{BMC,t}}/N_{\mathrm{BMC,r}}$ at the corresponding value of Γ. 3) Derive the black hole mass using the following equation

$$M_{\mathrm{BH,t}} = M_{\mathrm{BH,r}} \times (N_{\mathrm{BMC,t}}/N_{\mathrm{BMC,r}}) \times (d_t/d_r)^2 \times f_G \quad (1)$$

where $M_{\mathrm{BH,r}}$ is the black hole mass of the reference object, $N_{\mathrm{BMC,t}}$ and $N_{\mathrm{BMC,r}}$ are the respective normalizations for target and reference objects, d_t and d_r are the corresponding distances, and $f_G = \cos\theta_r/\cos\theta_t$ is a geometrical factor that depends on the respective inclination angles. The above formula is readily obtained by considering that a) the normalization is a function of luminosity and distance: $N_{\mathrm{BMC}} \propto L/d^2$; b) the luminosity can be expressed by $L \propto \eta M_{\mathrm{BH}} \dot{m}$, where η is the radiative efficiency, and c) assuming that different sources in the same spectral state (defined by the photon index) have the same η and $\dot{m}$.

To illustrate this method, in Figure 9 we show the $\Gamma - N_{\mathrm{BMC}}$ diagram for GRO J1655-40, which is the primary reference source since the parameters of this system are the most tightly constrained: $M_{\mathrm{BH}}/M_\odot = 6.3 \pm 0.3$, $i = 70^o \pm 1^o$, $d = 3.2 \pm 0.2$ kpc (Greene et al. 2001; Hjellming & Rupen 1995; but see also Foellmi et al. 2006 for a discording view on the distance of GRO J1655-40).

Since, unlike the first method from Shrader & Titarchuk, this method is relatively new and has never been tested before for AGNs or IMBHs, we apply it first to an AGN of known mass, as a check. We chose the broad-line

radio galaxy (BLRG) 3C 390.3 (z=0.056 corresponding to a luminosity distance of 247 Mpc), because, it has a well constrained mass as well as a well constrained disk inclination. One black hole mass estimate of $M_{\rm BH} = (5 \pm 1) \times 10^8$ M$_\odot$ is based on the velocity dispersion (Nelson et al. 2004; Lewis & Eracleous 2006) and another estimate of $M_{\rm BH} = (2.9 \pm 0.6) \times 10^8$ M$_\odot$ based on reverberation mapping (Peterson et al. 2004)– An inclination angle of $25^\circ < i < 35^\circ$ is derived from the radio data (Eracleous, Halpern & Livio 1996, Giovannini et al. 2001, Lewis et al. 2005), while an angle of $26^{\circ}{}^{+4^\circ}_{-2^\circ}$ is derived from the profiles of the double-peaked optical emission lines (Eracleous & Halpern 1994). Fitting the *XMM-Newton* EPIC pn spectrum of 3C 390.3 with the `BMC` model (and a Gaussian line to account for the Fe Kα emission), we obtain: $kT = 0.106 \pm 0.003$ keV, $\alpha = 0.75 \pm 0.01$, $\log(A) = 0.66 \pm 0.03$, and $N_{\rm BMC} = (8.7 \pm 0.2) \times 10^{-5}$. From Figure 6, we infer that at $\Gamma = 1.75$ the reference normalization is $N_{\rm BMC,r} \simeq 0.3$. Inserting this result and the corresponding quantities in equation (1) we obtain $M_{\rm BH} \simeq 1.5 \times 10^8$ M$_\odot$. Using $d_{\rm GROJ1655-40} = 1.7$ kpc, as suggested by Foellmi et al. (2006), the resulting mass increases by a factor ∼3.5, yielding $M_{\rm BH} \simeq 5 \times 10^8$ M$_\odot$, which is in good agreement with the accepted value.

Since the value of $M_{\rm BH}$ derived for 3C 390.3 is reasonably close to the estimates obtained from optical data, we can try to apply this procedure (hereafter method 2 for simplicity) and the Shrader & Titarchuk method (method 1) to the 2 X-ray enigmatic sources detected by *Chandra*. Using the results from the spectral fitting with the `BMC` model, for source B we obtain $M_{\rm BH} \simeq (1.4 \times 10^3 - 1.5 \times 10^4)$ M$_\odot$ and $M_{\rm BH} \simeq (3 \times 10^2 - 3.4 \times 10^3)$ M$_\odot$, using method 1 and method 2, respectively. The ranges of $M_{\rm BH}$ reflect the relatively large uncertainties of the spectral parameters. Similarly, for source C, the two methods yield respectively $M_{\rm BH} \simeq (1.8 \times 10^3 - 1.3 \times 10^4)$ M$_\odot$ and $M_{\rm BH} \simeq (2.3 \times 10^3 - 2 \times 10^4)$ M$_\odot$.

These findings are important for a number of reasons. First, the consistency between the BH mass estimates obtained with 2 different methods lends support to the validity of the 2 methods. Second, since the methods are independent, the mass obtained from one method can be used in the second method to verify the distance of the object, and the similarity between $M_{\rm BH}$ seems to confirm the hypothesis that the 2 enigmatic sources are located in NGC 3621. Finally, and perhaps most importantly, our analysis suggest the presence of 2 IMBHs within a few hundred parsecs from the center of the galaxy, which hosts a small SMBH. This result, if confirmed, may have important implications for our understanding of the formation process of supermassive black holes. Indeed, several theoretical models predict the existence of off-nuclear supermassive black holes, which eventually merge with the central SMBH (see, e.g., Volonteri & Madau 2008 and reference therein).

5. CONCLUSIONS

We have analyzed a 25 ks *Chandra* observation of the bulgeless galaxy NGC 3621 to investigate the basic X-ray properties of the putative AGN and of 2 bright X-ray sources detected ∼20″ away from the center. The main results can be summarized as follows:

- A weak X-ray source was detected at the center of the galaxy, lending support to the finding from IR and optical spectroscopic studies that NGC 3621 hosts an AGN. Unfortunately, the signal-to-noise ratio hampers any spectral study of the source. We therefore used PIMMS to infer the possible luminosity associated with the putative AGN. Assuming an absorbed power-law model with $\Gamma = 1.7 - 2$ and $N_{\rm H} = 5 \times 10^{21} - 5 \times 10^{23}$ cm^{-2}, the resulting luminosity is $L_{0.5-8\,{\rm keV}} \sim 7 \times 10^{37} - 3 \times 10^{39}$ erg s^{-1} ($L_{2-10\,{\rm keV}} \sim 5 \times 10^{37} - 2 \times 10^{39}$ erg s^{-1}), depending on the choice of intrinsic absorption.

- Combining the X-ray luminosity with information derived from recent IR and optical observations, and using several independent tests, we infer that a heavily absorbed AGN scenario is more likely for NGC 3621. If this is the case, exploiting the direct correlation between bolometric correction factor and Eddington ratio, we speculate that the AGN is in its early phase with a supermassive black hole of relatively small mass ($M_{\rm BH} \simeq 2 \times 10^4$ M$_\odot$) accreting at high rate ($L_{\rm bol}/L_{\rm Edd} \gtrsim 0.2$).

- The *Chandra* observation also reveals the presence of 2 bright off-nuclear sources located ∼20″ away from the central source. Direct fitting of the X-ray spectra indicates that both are well described by absorbed power laws with luminosities of the order of 10^{39} erg s^{-1}, in the hypothesis that they are located in NGC 3621.

- The lack of strong optical/UV counterparts and the intrinsic absorption argue against the 2 off-nuclear sources being Galactic objects that appear to be in NGC 3621 by chance superposition. Similarly, the combination of X-ray and optical measurements seems to rule out the hypothesis of background AGN. Assuming that these sources are at the distance of NGC 3621, leads to the conclusion that their luminosities exceed the Eddington limit for a neutron star and suggests that these are black holes.

- In order to discriminate between 2 competing scenarios for these putative black hole systems (namely, IMBHs, or bright microquasars similar to GRS 1915+105 in NGC 3621), we have applied 2 different methods that allow to determine the $M_{\rm BH}$-to-distance ratio, once the spectrum is fitted with the `BMC` model Comptonization model. Both methods consistently suggest that the 2 off-nuclear sources are located in NGC 3621 and have $M_{\rm BH}$ of a few thousand solar masses.

In conclusion, our *Chandra* observation has confirmed that NGC 3621 is an extremely interesting object. Not only do the X-ray data support the scenario that NGC 3621 hosts a buried AGN, but they also suggest the possible presence of 2 IMBHs located relatively close to the center of the galaxy. These findings may play a crucial role in our understanding of the connection between galaxy formation and SMBHs at their center, and of the process leading to the formation of the SMBH itself. It must be, however, kept in mind that these results were derived from

data with limited statistics. Therefore, deeper X-ray exposures from more sensitive instruments complemented with observations at longer wavelengths (with emphasis on the radio band that is largely unaffected by absorption) will be necessary to confirm and possibly further our main conclusions.

We thank the referee for the constructive comments and suggestions that improved the clarity of the paper. MG acknowledges support by the *Chandra* Guest Investigator Program under NASA grant GO8-9112X.

REFERENCES

Arnaud, K. 1996, in ASP Conf. Ser. 101, Astronomical Data Analysis Software and Systems V, ed. G. Jacoby & J. Barnes (San Francisco: ASP), 17
Barth, A.J., Greene, J.E., & Ho, L.C. 2008, AJ, 136, 1179
Barth, A.J., Strigari, L.E., Bentz, M.C., Greene, J.E., Ho, L.C. 2009, ApJ, 690, 1031
Bassani, L., et al. 1999, ApJS, 121, 473
Cox, A.N. & Allen, C.W. 2000, Allen's Astrophysical Quantities, IV edition (New York: AIP)
Dorman, B. & Arnaud, K.A. 2001 in Astronomical Data Analysis Software and Systems X, ASP Conference Proceedings, Vol. 238. Edited by F. R. Harnden, Jr., Francis A. Primini, and Harry E. Payne. San Francisco: Astronomical Society of the Pacific, p.415
Cash, W. 1979, ApJ 228, 939
de Jong, T., et al. 1984, ApJ, 278, 67
Desroches, L.-B & Ho, L.C. 2009, ApJ, 690, 267
Dewangan, G.C., Mathur, S., Griffiths, R.E., & Rao, A.R. 2008, ApJ, 689, 762
Dudik, R.P., et al. 2005, ApJ, 620, 113
Dudik, R.P., et al. 2007, ApJ, 664, 71
Eracleous, M. & Halpern, J. P. 1994, ApJS, 90, 1
Eracleous, M., Halpern, J. P., & Livio, M. 1996, ApJ, 459, 89
Ferrarese, L. & Merritt, D. 2000, ApJ, 539, L9
Filippenko, A.V. & Ho, L.C. 2003, ApJ, 588, L13
Flohic, H. M. L. G., Eracleous, M., Chartas, G., Shields, J. C. & Moran, E. C. 2006, ApJ, 647, 140
Foellmi, C., Depagne, E., Dall, T.H., Mirabel, I.F. 2006, A&A 457, 249
Freedman, W.L., et al. 2001,ApJ, 553, 47
Gebhardt, K., et al. 2000, ApJ, 539, L13
Gehrels, N. 1986, ApJ, 303, 336
Genzel, R. et al. 1998, ApJ, 498, 579
Giovannini, G., Cotton, W.D., Feretti, L., Lara, L., & Venturi, T. 2001, ApJ, 552, 508
González-Martín, O., Masegosa, J., Márquez, I., Guerrero, M. A., & Dultzin-Hacyan, D. 2006, å, 460, 45
Gorjian, V., et al. 2008, ApJ, 679, 1040
Greene, J., Bailyn, C.D., & Orosz, J.A. 2001, ApJ, 554, 1290
Greene, J.E. & Ho, L.C. 2004, ApJ, 610, 722
Greene, J.E. & Ho, L.C. 2007, ApJ, 670, 92
Ghosh, H., Mathur, S., Fiore, F., & Ferrarese, L. 2008, ApJ, 687, 216
Guainazzi, M., Fabian, A.C., Iwasawa, K., & Fiore, F. 2005, MNRAS, 356, 295
Heckman, T.M. 1980, A&A, 88, 311
Hjellming, R.M. & Rupen, M.P. 1995, Nature, 375, 464
Ho, L.C., Filippenko, A.V. & Sargent, W.L. 1997, ApJS, 112, 315
Kennicutt, R. C., Jr., et al. 2003, PASP, 115, 928
Lewis, K. T., Eracleous, M., Gliozzi, M., Sambruna, R. M., & Mushotzky, R. F. 2005, ApJ, 622, 816.
Lewis, K. T., & Eracleous, M 2006, ApJ, 642, 711
Marshall, H.L., et al. 2005, ApJS, 156, 13
Moran, E.C. et al. 2005, AJ, 129, 2108
Mulchaey, J.S., et al. 1994, ApJ, 436, 586
Nelson, C.H., Green, R.F., Bower, G., Gebhardt, K., & Weistrop, D. 2004, ApJ, 615, 652
Peterson, B.M., et al. 2004, ApJ, 613, 682
Peterson, B.M., et al. 2005, ApJ, 632, 799
Ritter, H. & Kolb, U. 2003, A&A, 404, 301
Satyapal, S., Sambruna, R.M., & Dudik, R.P. 2004, A&A, 414, 825
Satyapal, S.,Vega, D., Heckman, T., O'Halloran, B., Dudik, R. 2007, ApJ, 663, L9
Satyapal, S.,Vega, D., Dudik, R., Abel, N.P., Heckman, T., 2008, ApJ, 677, 696
Sauvage, M. & Thuan, T.X. 1994, ApJ, 429, 153
Schlegel, D. J., Finkbeiner, D. P., & Davis, M. 1998, ApJ, 500, 525
Shields, J.C., et al. 2008, ApJ, 682, 104
Shakura, N.I. & Sunyaev, R.A. 1973, A&A, 24, 337
Shaposhnikov, N. & Titarchuk, L. 2007, ApJ, 663, 445
Shaposhnikov, N. & Titarchuk, L. 2009, ApJ in press (arXiv:0902.2852)
Shrader, C.R.& Titarchuk, L. 1999, ApJ, 521, L121
Shrader, C.R.& Titarchuk, L. 2003, ApJ, 598, 168
Sirianni, M., et al. 2005, PASP, 117, 1049
Skrutskie, M. F., et al. 2006, AJ, 131, 1163
Steffen, A.T., et al. 2006, AJ, 131, 2826
Sturm, E., et al. 2002, A&A, 393, 821
Thornton, C.E., Barth, A.J., Ho, L.C., Rutledge, R.E., & Greene, J.E. 2008, ApJ, 686, 892
Titarchuk, L.G., Mastichiadis, A. & Kylafis, N.D. 1997, ApJ, 487, 834
Titarchuk, L.G. & Fiorito, R. 2004, ApJ, 612, 988
Vasudevan, R.V., & Fabian, A.C. 2009, MNRAS, 392, 1124
Volonteri, M., Lodato, G., & Natarajan, P. 2008, MNRAS, 383, 1079
Volonteri, M. & Madau, P. 2008, ApJ, 687, L57

Table 1
Possible optical counterparts of off-nuclear X-ray sources

Source	RA (J2000)	DEC (J2000)	Offset (")	F_ν (F435W) (μJy)	F_ν (F555W) (μJy)	F_ν (F814W) (μJy)
B	11:18:15.180	-32:48:40.39	0.33	1.8 (2.5) ± 0.4	1.4 (1.8) ± 0.5	<4.5 (<5.2)
C1	11:18:18.248	-32:48:53.29	0.37	0.52 (0.72) ± 0.06	0.46 (0.59) ± 0.06	0.74 (0.85) ± 0.16
C2	11:18:18.252	-32:48:52.56	0.52	<0.19 (<0.26)	<0.17 (< 0.22)	0.52 (0.60) ± 0.16

The limits of the monochromatic fluxes are 3 sigma. The pivot wavelengths of the filters are respectively 4318 Å (for F435W), 5360 Å (for F555W), and 8060 Å (for F814W). Extinction corrected (based on Schlegel et al. 1998 maps) values are indicated in parentheses.

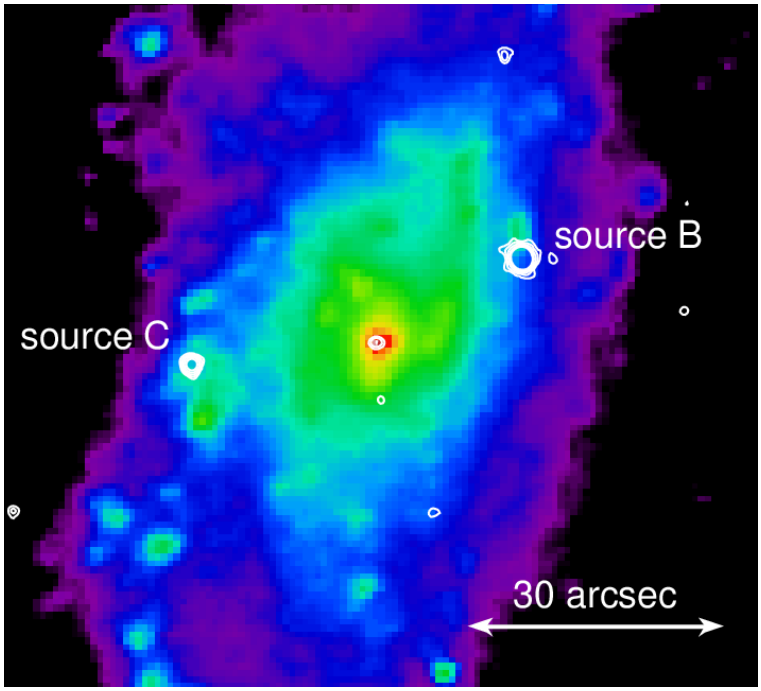

FIG. 1.— Spitzer IRAC 3.6μm image of the NGC 3621 galaxy from the SINGS survey (Kennicutt et al. 2003) overlaid with contours showing the *Chandra* X-ray point sources.

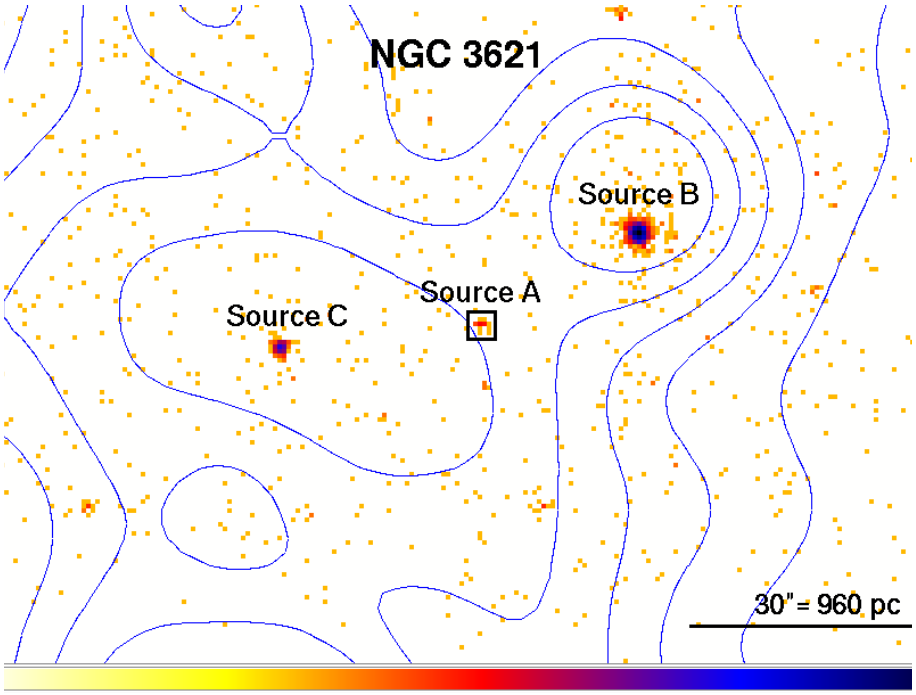

FIG. 2.— *Chandra* ACIS-S image of NGC 3621 in the 0.5–8 keV band with 1.4 GHz contours from a short VLA observation overlaid. The center of the galaxy, source A, is shown by the black box. Two off-nuclear bright sources, source B and source C, are located at $\sim 20''$ from the center.

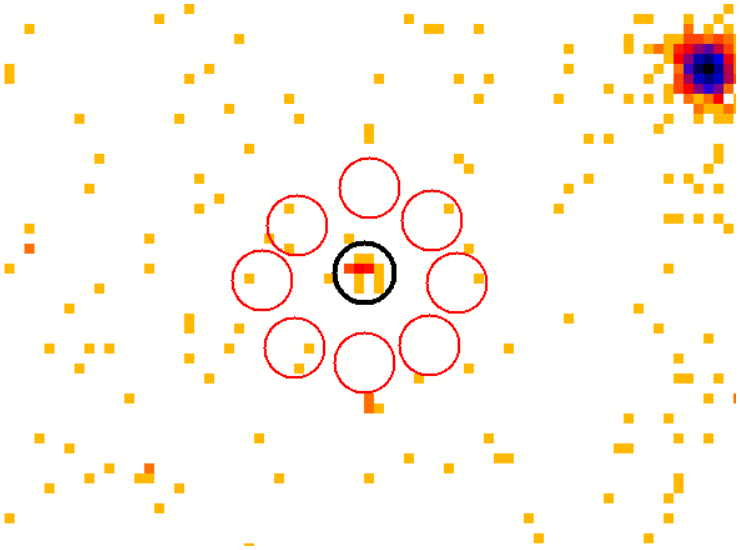

FIG. 3.— *Chandra* ACIS-S image of NGC 3621. The extraction region for the central source is indicated by the black thick circle. The surrounding circles are the background regions.

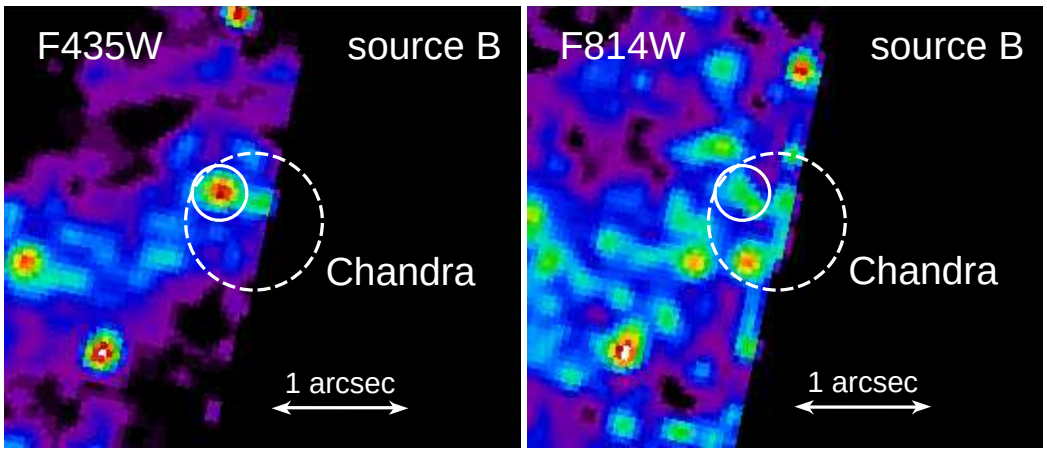

FIG. 4.— *HST* ACS WFC images (in 2 of the 3 observed bands) centered around the position of Source B, the brightest X-ray off-nuclear that is indicated with r=0.5" dashed circles. The images were smoothed with a Gaussian with $\sigma = 2$ pixels (0.098"). The edge of the WFC field of view is obvious in all images with only about ∼1/2 of the Chandra source B circle covered. Detected optical sources tabulated in Table 1 are indicated with solid r=0.2" circles.

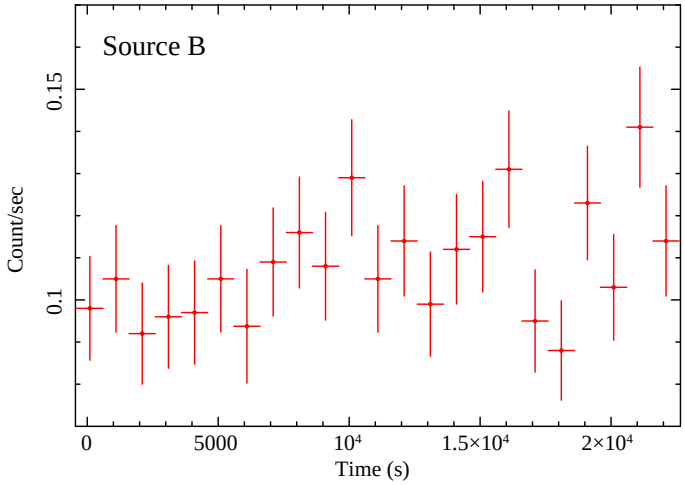

FIG. 5.— *Chandra* ACIS-S light curve of source B in the 0.5–8 keV energy band; time bins are 1000 s.

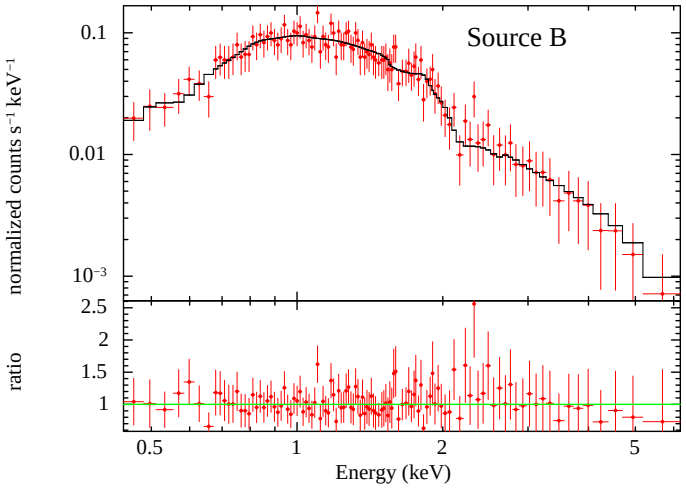

FIG. 6.— Spectrum of source B and data/model ratio to a simple power-law model modified by intrinsic photoelectric absorption.

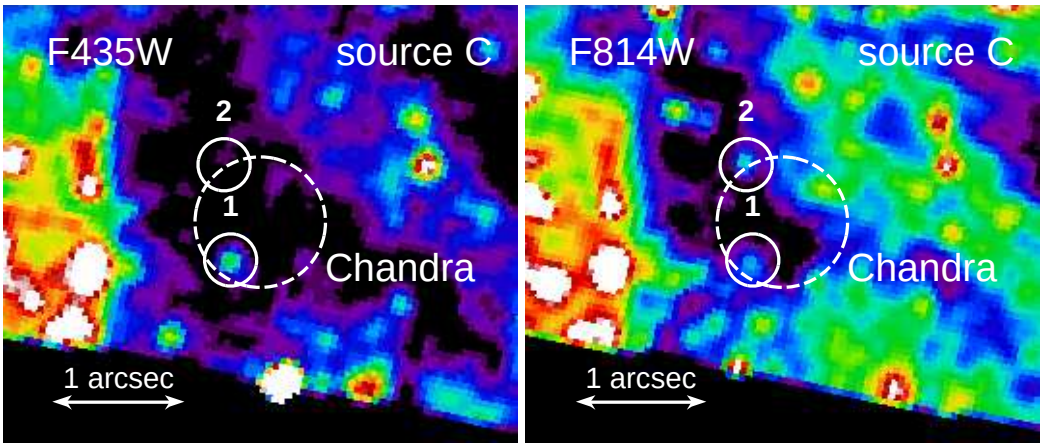

FIG. 7.— *HST* ACS WFC images (in 2 of the 3 observed bands) centered around the position of Source C, indicated with r=0.5" dashed circles. The images were smoothed with a Gaussian with $\sigma = 2$ pixels (0.098"). Detected optical sources tabulated in Table 1 are indicated with solid r=0.2" circles.

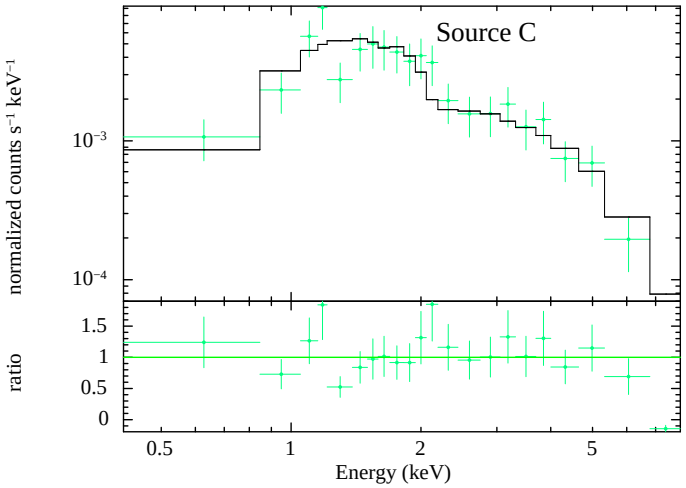

FIG. 8.— Spectrum of source C and data/model ratio to a simple power-law model modified by intrinsic photoelectric absorption.

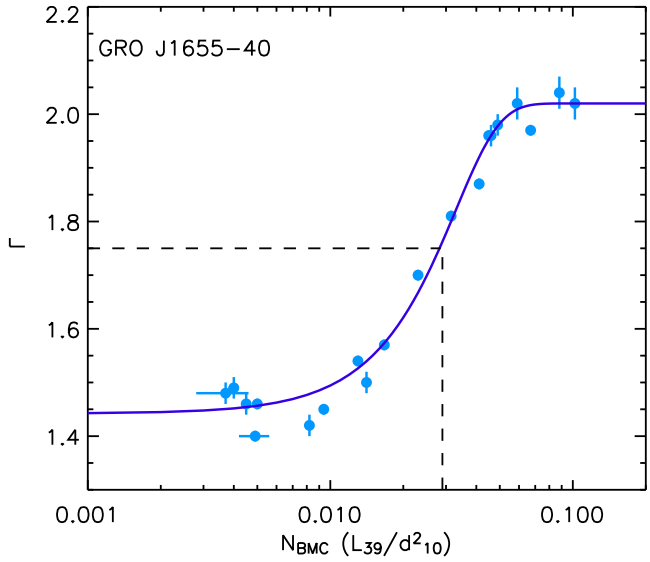

FIG. 9.— Photon index plotted versus the normalization of the BMC model for the microquasar GRO J1655-40 during the decay of the 2005 outburst (adapted from Shaposhnikov & Titarchuk (2008). The thick continuous line represents the best fitting function of the spectral trend. The dashed lines illustrate how we determine the value of $N_{\rm BMC,r}$ that we use in equation (1) to estimate the black hole mass of the BLRG of 3C 390.3.